DETAILED STABILITY ANALYSIS ON A MAJOR SLIDE OCCURRED NEAR UYILATTI WATERFALL, KOOKALTHORAI TO KOTAGIRI ROAD, THE NILGIRIS DISTRICT, TAMIL NADU

Abdul Kalam Azad H[1], Prasanna Venkatesh S[1], Lakshmi Narasimhan C[1], and Saranaathan S. E[2*]

[1]Department of Geology, Anna University, Chennai – 600025, India.

[2*]School of Civil Engineering, SASTRA Deemed University, Thanjavur – 613402, India. **(Corresponding Author)**

ABSTRACT. Landslides threaten hill stations like Ooty in the Nilgiris district of Southern India due to their steep terrain, heavy rainfall, and anthropogenic activities like improper planning and deforestation. In December 2022, a major landslide occurred on the Kokalthorai to Kotagiri road near Uyilatti waterfalls in Kotagiri taluk, Nilgiris district, Tamil Nadu. A study has been initiated through a comprehensive slope stability analysis, and the research methodology incorporates a combination of geotechnical investigations and field surveys. The rock slope stability assessment used geomechanical analysis systems, specifically the Rock Mass Rating (RMR) and Slope Mass Rating (SMR). The type of failure and their Factor of Safety (FOS) for individual discontinuities in rock slopes were calculated using the Hoek and Bray method. The FOS was computed using a Circular Failure Chart (CFC) regarding soil slopes. A detailed field investigation was conducted to collect data required for RMR and SMR calculation. As per Hoek and Bray's Kinematic methods, FOS was calculated. In this study, joint J3 satisfies the plane failure, and joint J2 and J3 are considered for wedge failure analysis. The details are furnished in this paper. Three surface soil samples and one core sample were collected to fulfill the study and calculated 'c' and 'phi' values using the Tri-axial shear test. The FOS was calculated by the CFC method. The analysis assessed the Factor of Safety (FOS) in three static conditions: dry, partially saturated, and completely saturated. The results indicate that the slopes in two sections (U and M) are unstable (FOS < 1), whereas the third section (L) is stable (FOS = 1.0). Urgent and targeted interventions are necessary to address the instability of the slopes, especially after the rainy season, to mitigate the risk of recurring and frequent failures on the hill.

KEYWORDS: *Slope Mass Rating, Kinematic analysis, Circular Failure Chart method, Factor of Safety, Stability analysis.*

1 Introduction

Landslides represent a significant natural hazard in hilly regions, in India (Aleotti and Chowdhury 1999), especially in the Nilgiris district of Tamil Nadu, influenced by the region's intricate geological formations and intense monsoonal rainfall. The Nilgiris, renowned for their picturesque landscapes and steep hills, are susceptible to slope instability and landslides. Factors such as heavy rainfall, soil type, slope angle, and human activities contribute to the heightened landslide risk in this area. Studies have shown that landslides in the Nilgiris district have resulted in the loss of lives, damage to infrastructure, and disruption of transportation networks. The Nilgiris district in Tamil Nadu is acknowledged for its

elevated susceptibility to landslides, as revealed by India's landslip hazard zonation atlas. This comprehensive atlas is meticulously crafted by the Building Materials and Technology Promotion Council (BMTPC), operating under the auspices of the Government of India. Unfortunately, in recent times, there has been a notable increase in the loss of life and property damage attributed to landslides in the Nilgiris hills. Kotagiri, a town panchayat in the Nilgiris District of Tamil Nadu, has recently faced a devastating landslide due to heavy rainfall and unstable terrain. The region's hilly topography and intense monsoon rains can lead to soil saturation, triggering landslides in vulnerable areas. Deforestation, improper land-use practices, and inadequate drainage systems may exacerbate the risk. In the event of a landslide in Kotagiri, significant damage to infrastructure, loss of property, and potential threats to human lives are significant concerns. This article focuses on the geotechnical assessment and examination of instability at a recent landslide located near Kokalthorai to Kotagiri road, close to Uyilatti waterfalls, Kotagiri Town Panchayat. Recognizing the critical importance of addressing landslide risks in the region, our research not only aims to provide a comprehensive analysis of the geotechnical factors contributing to landslides but also strives to contribute valuable insights for effective landslide mitigation strategies. By identifying the specific triggers and understanding the local geotechnical conditions that led to the major slide, the project provides essential insights for risk assessment and hazard zonation. The findings contribute to the design of targeted mitigation measures, including slope stabilization techniques, improved drainage systems, and vegetation management.

2 Methodology

2.1 Study Area

Kotagiri is a Hilltown and a taluk in The Nilgiris District. The name 'Kota-giri' itself means 'mountain of the Kotas'. Kotagiri is a panchayat town located at 11.43°N 76.88°E, east of the Nilgiris district in Tamil Nadu. The town has developed around numerous knolls and valleys. Kotagiri climate is classified as tropical. In Kotagiri, the quantity of rainfall during summers surpasses that of winters. In Kotagiri, the average annual temperature is 20.8 °C. About 1514 mm of precipitation falls annually. Precipitation is the lowest in January, with an average of 24 mm. On average, the highest rainfall occurs during June; with a mean value of 209 mm. Kotagiri is situated around 1847 meters above MSL. At the end of December 2022, a major landslide occurred on the Kokalthorai to Kotagiri road near Uyilatti waterfalls in Kotagiri panchayat town. **Figure 1** shows the location of Kotagiri. Geologically, the Nilgiris are integral to the Archean continental landmass of the Indian peninsula, primarily composed of pre-Cambrian metamorphic rocks such as gneisses, charnokite, and schist.

2.2 Geo-mechanical Analysis (RMR)

The Geo-mechanical classification system, also known as the Rock Mass Rating (RMR), is a classification method for assessing the quality of a rock mass. It was developed by the South African Council for Scientific and Industrial Research (CSIR) and is particularly applicable to excavations in the mining industry (Beiniawski, 1973). Over the years, several modifications have been made in 1976,

1979, and 1989. The current research is based on the 1989 version of this classification system. One notable advantage of the RMR system is its utilization of five parameters related to the geometry and mechanical conditions of the rock mass. In the RMR system, these parameters include:

- Strength of rock
- Rock Quality Designation (RQD)
- Spacing of discontinuities
- Condition of discontinuities
- Water inflow through discontinuities

Based on the earlier parameter, the RMR_{basic} rating attains a maximum value of 100. This maximum rating is categorized into five distinct classes: very good rock (80–100), good rock (60–80), fair rock (40–60), poor rock (20–40), and very poor rock (0–20). These findings are presented to facilitate an in-depth investigation into rock conditions ranging from fair to deplorable.

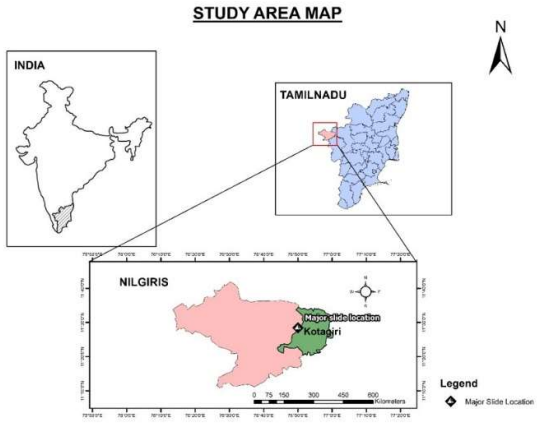

Figure 1 Location Map

2.3 Slope Mass Rating (SMR)

The Slope Mass Rating (SMR) system, introduced by Romana in 1985, is a classification method derived from Rock Mass Rating (RMR). It is designed to evaluate slope instability, incorporating risk parameters that consider the orientation of discontinuities and slopes, failure modes (planar, wedge, and toppling), and methods of slope excavation. The stability of rock slopes is influenced by factors such as the height and angle of slopes, disposition of geological discontinuities, material friction angle, material cohesion, and the impact of water pressure. Modifying these slopes involves studying rock formations' arrangement, the joints' intensity, and their correlation with planned excavation. The SMR is derived from RMR by introducing a factorial adjustment factor dependent on the excavation method. The formula for the final calculation is expressed as

$$SMR = RMR_{basic} + (F1 \times F2 \times F3) + F4 \quad (1)$$

where,

F1 considers the parallelism between joints and the strike of the slope face.

F2 relates to the dip angle of joints in the planar mode of failure, representing the probability of joint shear strength.

F3 reflects the relationship between the slope face and joint dip, with fair conditions when they are parallel. Conditions become unfavorable when the slope dips 10° more than the joints.

F4—involves the technique of excavation.

The stability classification comprises five distinct classes: totally unstable (<20), unstable (20–40), partially stable (40–60), stable (60–80), and fully stable (80–100). The study results provide initial insights for conducting a comprehensive investigation into specific planar and wedge discontinuities in the rock section. The density and unit weight of the rock sample were determined using the ISRM (1981) procedure, adapted to the American Society for Testing Materials (ASTM 1994).

2.4 Kinematic Analysis

Kinematic analysis is a technique used to assess potential modes of rock slope failures, explicitly focusing on plane, wedge, and toppling failures induced by unfavorably oriented discontinuities. These discontinuities include joints, faults, bedding planes, foliation, and shear zones, serving as potential planes of failure. The method relies on Markland's test, as outlined in Hoek and Bray (1981), and employs stereonet plotting to determine the type of failure. In the context of kinematic analysis, planar failure occurs when a position is assumed along continuous joints dipping towards the slope, with a strike nearly parallel to the slope face. Wedge failures, more common than planar failures, manifest along two joints in different directions, dipping towards the slope. Toppling failures, on the other hand, occur along continuous joints that dip against the slope, with a strike parallel to the slope face. Notably, toppling failures develop gradually and are less susceptible to sudden collapses. The Brunton compass measures dip and strike in assessing cut-slope joints and fractures. The stability analysis of the slope is then calculated using a stereo net for plotting plane poles and dip vectors, as outlined by Hoek and Bray (1981). This analytical approach, also known as the graphical representation of joints and slope data on the equal area/angle stereo net, visually depicts potential failure points. This straightforward method provides an initial indication of possible failure, serving as a crucial tool in structural geology. The significance of this technique lies in its ability to represent and analyze three-dimensional orientation data of joints and slope faces in a two-dimensional format. Similarly, debris instability analysis of hill slopes has been studied by many authors (Sharma et al. 2013; Saranathan et al. 2014; Saranaathan and Kannan 2017; Siddique et al. 2020; Kamal et al. 2023; Prasanna Venkatesh et al. 2023). By eliminating one dimension from consideration, lines and points can effectively portray the plan and lines, respectively.

Plane failure is infrequent in rock sections, with geometric conditions typically triggering actual slope failures. The safety factor for rock slopes in ghat sections is determined using Hoek and Bray's simplified equation (Eq. 2). Once the parameters of joint plane inclination and water penetration are identified, calculating the safety factor becomes straightforward.

$$F = (2c/\gamma H)\times P + \{Q\times \cot\psi_p - R(P+S)\} / Q + R\times S \cot\psi_p \quad (2)$$

The factors P, Q, R, and S are non-dimensional ratios.

Rock sections experience planar failures when they slide along a sloping plane, whereas wedge failures occur at the sloping summit, where slides follow the intersections of two joint sections. The derivation of the safety factor (Eq. 3) relies on the assumptions put forth by Hoek and Bray.

$$F = \{3/\gamma H\,(c_A.X + c_B.Y)\} + \{(A - (\gamma_w/2\gamma).X)\}\tan\phi_A + (B - (\gamma_w/2\gamma).Y)\tan\phi_B \quad (3)$$

The factors X, Y, A, and B in Eq. (3) are non-dimensional ratios.

2.5 Circular Failure Chart (CFC) Method

In the context of rock slopes, geological features play a crucial role in disaster mitigation. Conversely, in the case of soil, the absence of a distinct structural failure outline allows the displacement surface to fail freely along the slope. The circular failure chart method (Hoek and Bray 1981; Kannan et al. 2017) is a simple method for studying soil slope stability using the available standard charts depending on the existing field condition. The Circular Failure Chart (CFC) was computed using a Hewlett—Packard 91,008 calculator (Hoek and Bray 1981), with charts numbered 1 to 5 corresponding to different groundwater conditions (**Figure 2a**). The stages of the failure outline are presented to determine the safety factor for a soil slope using equations and the geotechnical parameters specific to the soil slope. The dimensionless relation can be established at each chart's fringe, and the radial line's intersection with the resultant slope inclination can be calculated. This intersection provides the safety factors for X and Y; the average safety factor is also computed (**Figure 2b**). The fundamental geo-mechanical properties of rock and soil were identified to facilitate the analysis. The detailed flow chart is furnished in **Figure 3.**

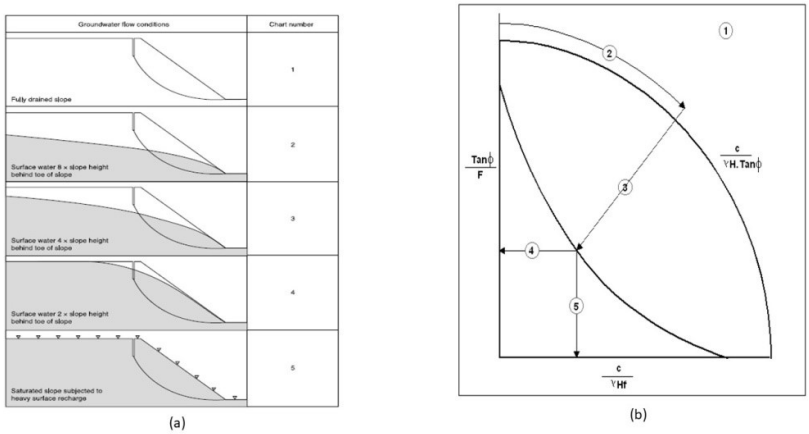

Figure 2(a) Illustrates CFC conditions about Groundwater flow. **(b)** Outlines the calculation of the Factor of Safety from the CFC

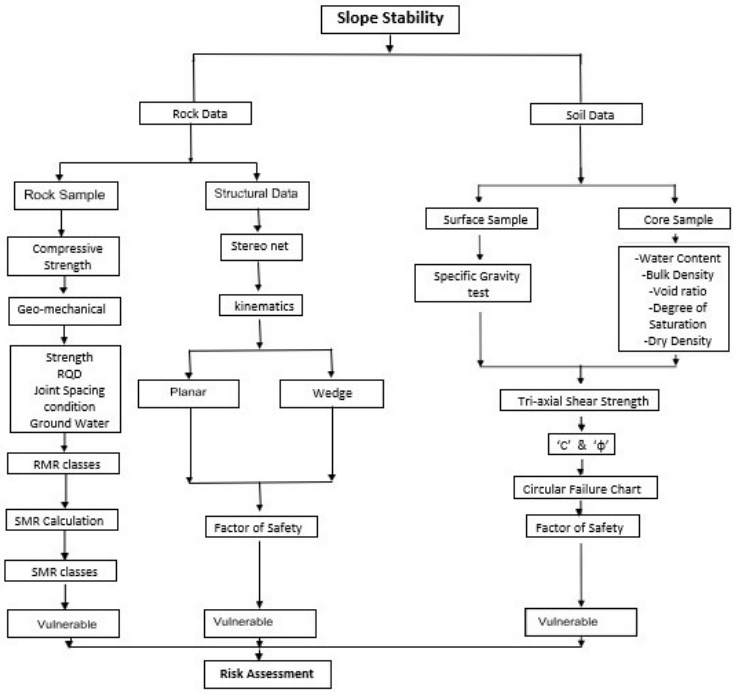

Figure 3 Flow Chart (Prasanna Venkatesh et al. 2023)

3 Results and Discussion

3.1 Rock Mass Rating

The method of rock mass rating is discussed in section 3.1. Three rock discontinuities were identified for RMR studies. For this study, the in-situ compressive strength of rock was determined using a Schmidt Rebound hammer in the field. Additionally, two representative lump rock samples were collected from the field to determine compressive strength by IS 8764:1998 (Anon 1998), utilizing the Point Load Test Index. The calculations of compressive strength for the rock samples are presented in **Table 1**, with point load index values ranging from 3.2312 MPa to 3.5617 MPa. **Table 2** displays the RMR parameters of the rock sections collected from the field visit. Based on these parameters, the rock mass rating values and overall ratings are shown in **Table 3**. A review of the RMR values indicates a range from 58 to 62. Out of the three rock discontinuities, one falls under Class II, indicating good rock, and two under Class III, signifying fair rock condition.

Table 1 Point Load Test Index (IS 8764:1998)

S.No.	Sample ID	**Peak Load in KN**	**Width in cm**	**Distance between Load points in cm**	**DW in cm^2**	**Strength in Kgf/cm^2**	**Strength in Mpa**
1	T1	14.5	10.1	5.4	54.54	32.9496	3.2312
	M1	15	8.64	5.8	50.112	36.3200	3.5617

Table 2 RMR parameters of rock sections

Slope Location : 11o28'27"N 76o50'01"E			
Rock Type: Gneissic rock			
Height of slope: 20 m			
RMR Parameters			
	J1	J2	J3
1. CS (Mpa)	3.395		
2. RQD	50% - 75%		
3. Joint Spacing	20	15	20
4. Joint Conditions			
a. Discontinuity Length	10 - 20 m	10 - 20 m	3 - 10 m
b. Separation	>5 mm	1 - 5 mm	1 - 5 mm
c. Roughness	Rough	Rough	Slightly Rough
d. Infilling	Hard filling <5 mm	Hard filling <5 mm	Hard filling <5 mm
e. Weathering	Slightly Weathering	Slightly Weathering	Slightly Weathering
5. Groundwater	Wet	Wet	Wet
6. Orientation of Joint			
Slope direction - N 237 Natural slope - 37 Cut slope - 63	48/14	142/81	215/49
Reference/Date	Abdul Kalam Azad H and Prasanna Venkatesh S 25.06.2023		

Table 3 The overall ratings have been obtained for RMR.

RATING			
	J1	**J2**	**J3**
1. Co (Mpa)	7	7	7
2. RQD	13	13	13
3. Joint Spacing	20	15	20
4. Joint Conditions			
Discontinuity Length	1	1	2
Separation	0	1	1
Roughness	5	5	3
Infilling	4	4	2
Weathering	5	5	5
5. Ground Water	7	7	7
6. Orientation of Joints	**48/14**	**142/81**	**215/49**
ROCK MASS CLASSES DETERMINED FROM TOTAL RATINGS			
TOTAL RATING	**62**	**58**	**60**
CLASS	**II**	**III**	**III**
DESCRIPTION	**GOOD ROCK**	**FAIR ROCK**	**FAIR ROCK**

3.2 Slope Mass Rating

The procedure for determining slope mass ratings was discussed in section 3.2. The slope mass rating of each slope is computed using the equation provided by Romana (1985) and modified by Anbalagan et al. (1992), which has been adopted as the BIS code (IS: 13365 Part 3, 1998). It depends on parameters such as RMR_{basic}, F1, F2, F3, and F4. SMR values vary for different failures in a particular slope due

to the differing ratings of F1, F2, and F3, even when RMR and F4 are the same. Therefore, it is necessary to judiciously explore all possible failure modes and calculate the corresponding SMR values for the slope. The SMR classes and corresponding stability can be obtained from the stability classes (**Table 4**) provided by Romana (1985). Five stability classes range from class I, indicating an utterly stable slope, to class V, indicating a precarious slope. The SMR calculation of J3 stability has been given in **Table 5**.

Table 4 Description of SMR classes – BIS code (IS: 13365 Part 3 1997)

Class No.	**V**	**IV**	**III**	**II**	**I**
SMR rating	0-20	21-40	41-60	61-80	81-100
Description	Very bad	Bad	Normal	Good	Very good
Stability	Completely stable	Unstable	Partially stable	Stable	Completely stable
Failures	Big planar or soil-like	Planar or big wedges	Some joints or many wedges	Some blocks	None

Table 5 Slope Mass Rating calculations for J3 Joint

Parameters	**J3**
αj	N215°
βj	49°
αs	N237°
βs	63°
$\lvert\alpha j - \alpha s\rvert$ = F1	0.4
$\lvert\beta j\rvert$ = F2	1.00
$\beta j - \beta s$ = F3	-60
F4	0
RMR	
SMR = RMR_{basic}+(F1. F2. F3) + F4	
SMR	**36**
Class No	**IV**
Description	**Bad**
Stability	**Unstable**
Failure	**Planar or big wedges**

3.3 Kinematic analysis

Analysis of Plane Failure

According to Markland's test, a slope has a high probability of plane failure if it satisfies $\psi s > \psi p > \phi$. This rock section is located at 11°28'27" N latitude and 76°50'01" E longitude. The rocks are predominantly exposed, and highly jointed gneiss rock is present on this slope. The cut slope height is about 6m. Three sets of joints, J1, J2, and J3, are present in this slope. On the upper slope, a forest and

an artificial canal are observed, while on the lower slope, there is a tea plantation. The joints are exposed throughout the slope. J2 fulfills the planar analysis, with the discontinuity in the N142° dip direction and an inclination of 81° (**Figure 4**). The safety factor was calculated according to Hoek and Bray's equation 2. As per the planar analysis, the factor of safety for this slope is 1.583, 0.5260, 0.2455, and 0.1637 for dry, 50% saturation, 25% saturation, and fully saturated conditions, respectively. The calculations are shown in **Table 6**. Some rock falls have already occurred on this slope in 2022, and it is unstable in moderate to heavy rainfall.

Table 6 Planar Calculation

Section ID	Input Data	Function value	Calculations using formula	Results
J2	$\psi_p = 49°$ $\psi_f = 37°$ $\gamma = 2.78$gm/cc $\gamma_w = 1$gm/cc z = 2000cm c = 2957.177gm/cc H = 2000cm	$Cosec\psi_p = 1.3250$ $Cot\psi_p = 0.8692$ $Cot\psi_f = 1.3270$ $Sin\psi_p = 0.7547$ $\gamma_w/\gamma = 0.3597$ $z_w/z = 1.0;0.5;0.25;0$ z/H = 1.0000 $2c/\gamma H = 1.0637$	$P = (1 - z/H).\ cosec\psi_p$ $= 0 \times 1.3250 = 0$	**P = 0**
			$Q = \{(1 - (z/H)^2)\ cot\psi_p - cot\psi_f\}\ sin\psi_p$ $= -1.3270 \times 0.9876 = -1.3105$	**Q = -1.3105**
			When, zw/z = 1; $R = \gamma_w/\gamma.\ z_w/z\ .$ z/H = 0.3597	**R=0.3597**
			When, zw/z = 0.5; $R = \gamma_w/\gamma.\ z_w/z\ .$ z/H = 0.1799	**R= 0.1799**
			When, zw/z = 0.25; $R = \gamma_w/\gamma.\ z_w/z\ .$ z/H = 0.0449	**R=0.0449**
			When, zw/z = 0; $R = \gamma_w/\gamma.\ z_w/z\ .$ z/H = 0	**R=0**
			When zw/z = 1; $S = z_w/z\ .\ z/H\ .\ sin\psi p$ = 0.7547	**S = 0.7547**
			When zw/z = 0.5; $S = z_w/z\ .\ z/H\ .\ sin\psi p$ = 0.3773	**S =0.3773**
			When zw/z =0.25; $S = z_w/z\ .\ z/H\ .\ sin\psi p$ =0.1886	**S =0.1886**
			When zw/z = 0; $S = z_w/z\ .\ z/H\ .\ sin\psi p$ = 0	**S =0**
Case 1: when zw/z = 1, i.e., When the tension crack is filled with water (Zw=Z), FoS = 0.1637				
Case 2: when zw/z = 0.5, i.e., When the tension crack is filled with 50% of water, FoS = 0.2455				
Case 3: when zw/z = 0.25, i.e., when the tension crack is filled with 25% of water, FoS = 0.5260				
Case 4: when zw/z = 0, i.e., when the tension crack is dry, FoS = 1.583				

Analysis of Wedge Failure

The failure of a slope, wherein structural features that facilitate sliding run across the slope crest and sliding occurs along the line of intersection of two such planes, is termed a Wedge failure. This section is situated at 11°28'27" N latitude and 76°50'01" E longitude. Gneiss is prevalent in this zone, as identified during field investigation. Tension cracks or joints are visible in the upper slope, with three sets of joints, namely J1, J2, and J3, present in this slope. Joint 2 and Joint 3 fulfill the Hoek and Bray conditions for wedge analysis, as illustrated in **Figure 4**. The cross section of the slope presented in **Figure 5.** The plunge direction is N215°, and the dip is approximately 48°, nearly exposed in the cut slope. According to the analysis, the safety factor for the slope is approximately 0.4785, as detailed in **Table 7**. The safety factor is just below one, indicating an unstable slope.

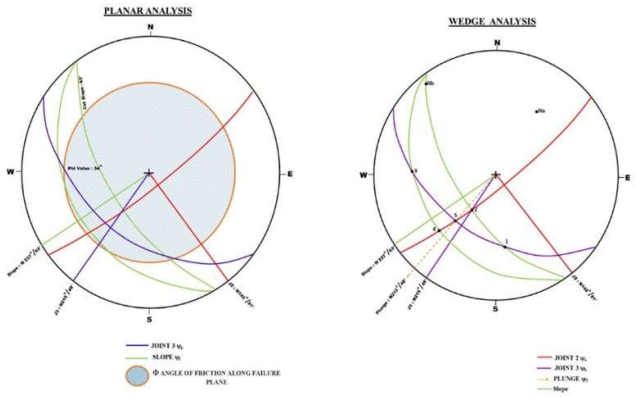

Figure 4 Stereonet analysis for Planar and Wedge Failure analysis

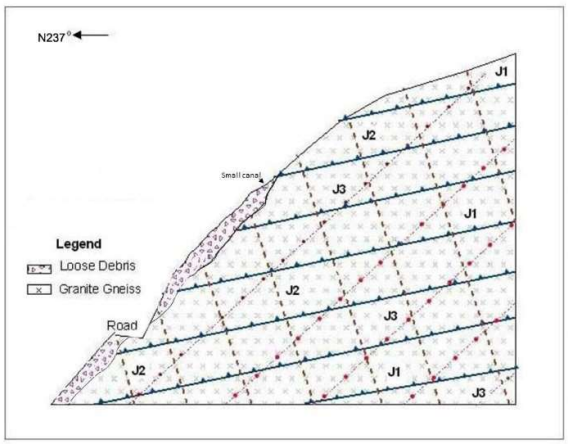

Figure 5 Cross-section of the slope

Table 7 Wedge Calculation

Section ID	Input Data	Function Value	Calculations using formula	Results
J2-J3	$\psi_a = 49°$ $\psi_b = 81°$ $\psi_5 = 48°$ $\theta_{na.nb} = 70°$	$Cos\psi_a = 0.6560$ $Cos\psi_b = 0.1564$ $Sin\psi_5 = 0.7341$ $Cos\theta_{na.nb} = -0.3420$ $Sin\theta_{na.nb} = 0.9397$	$A = Cos\psi_a - Cos\psi_b.Cos\theta_{na.nb} / Sin\psi_5.Sin^2\theta_{na.nb}$ $= -0.16/0.64 = -0.25$ $B = Cos\psi_b - Cos\psi_a.Cos\theta_{na.nb} / Sin\psi_5.Sin^2\theta_{na.nb}$ $= 0.59/0.64 = 0.92$	A = -0.25 B = 0.92
	$\theta_{24} = 38°$ $\theta_{45} = 12°$ $\theta_{2na} = 88°$	$Sin\theta_{24} = 0.61566$ $Sin\theta_{45} = 0.2079$ $Cos\theta_{2na} = 0.0348$	$X = Sin\theta_{24} / Sin\theta_{45}.Cos_{2.na} = 0.61/ 0.20*0.034 = 0.1$	X = 0.1
	$\theta_{13} = 92°$ $\theta_{35} = 53°$ $\theta_{1nb} = 134°$	$Sin\theta_{13} = 0.9993$ $Sin\theta_{35} = 0.7986$ $Cos\theta_{1nb} = -0.6945$	$Y = Sin\theta_{13} / Sin\theta_{35}.Cos_{1.nb} = 0.99/ 079*-0.69 = -1.816$	Y = -1.816
	$\phi_A = 34°$ $\phi_B = 34°$ $\gamma = 2.78gm/cc$ $\gamma_w = 1$ $c_A = c_B = 295.2gm/cc$ H = 2000cm	$Tan\phi_A = 0.700$ $Tan\ \phi_B = 0.700$ $\gamma = 2.78gm/cc$ $3/\gamma H = 0.00053$	$F = \{3/\gamma H (c_A.X + c_B.Y)\} + \{(A – (\gamma_w/2\gamma).X)\}tan\phi_A + (B – (\gamma_w/2\gamma).Y) tan\phi_B$ $= 0.00018-0.1685+0.64704$ $=0.4785$	F = 0.4785

3.4 CFC Analysis

In the Kokalthorai to Kotagiri ghat section area, the cut slope developed for road construction plays a crucial role in identifying the soil thickness for circular or talus failure. The cut slope heights are less than 5m, and soil predominates in the upper levels of this zone. Given this, it is assumed that talus failure patterns may dominate where the thickness is less than 5m and follow a circular pattern where the thickness exceeds 5m. Three soil slope samples were collected for study, with three samples collected from each at different heights (Upper, Middle, and Lower - U, M, L) after cleaning the topsoil to a depth of two feet in the specific location. Tri-axial shear tests (unconfined and undrained Tests) were conducted on these samples, and the average density (ρ) of the soil materials obtained from core cutter samples in the field is detailed in **Table 8**. Tri-axial shear tests with three different normal loads provided shear strength values. They were plotted to obtain representative shear strength parameters in normal stress (x-axis) versus shear stress (y-axis). Cohesion (c) and friction angle (ϕ) values for Mohr's circle calculation were derived from the best-fit lines of shear test results. The tri-axial shear test followed the procedure outlined in IS: 2720, and the laboratory results are provided in **Table 9**. Soil section details for the location are summarized in **Table 10**.

Table 8 Core Cutter Result IS: 2720 (Part 29) – 1985

S. No	Sample No	S1
1	Weight of core cutter (W1) kg	0.934
2	Weight of soil + core cutter (W2) kg	2.373
3	Weight of soil (W2- W1) g	1439
4	Volume of core cutter(V) m^3	$1.02\times10^{-3}m^3$
5	The in-situ density of the soil (ρ) g/cm^3	1.410

The factor of safety, determined through the CFC technique under different groundwater levels, is provided in **Table 11**. The findings indicate that slopes U and M are unsafe, and L is partially stable. Moreover, it is noteworthy that all soil sections exhibit instability, particularly in the face of intense rainfall.

Table 9 Tri-axial Shear Test Results

S. No	Soil section	Cell pressure (kg/cm2)	Deviator stress (KN)	Normal stress (KN)	Cohesion of soil (kPa)	Angle of shearing resistance (°)
1	U	1	2.172775689	3.172775689	4.8946	26.791°
2		1.5	2.871240602	4.371240602		
3		2.0	3.65914787	5.65914787		
4	L	1	3.004385965	4.004385965	4.9135	25.63°
5		1.5	3.834586466	5.334586466		
6		2.0	4.542606516	6.542606516		
7	M	1	10.43859649	11.43859649	32.6309	21.054°
8		1.5	11.10432331	12.60432331		
9		2.0	11.62280702	13.62280702		
Note: **The tri-axial shear test has been conducted per the technique given in BIS: 2720**						

Table 10 Soil Section details

Slope location	Northing: 11°28'29" N Easting: 79°49'59.137" E
Height (m)	20.2
Slope	Direction-dip amount: N 251°-45° Cut slope dip amount: 79°
Description	• Top of the slope covers small bushes 2to5 m • Canal is flowing in the N-S direction • Below road tea garden • no support measures are found • Soil wet condition below 1m. This is due to seepage of the canal due to bison movement.
Soil Characteristics	Brownish soil
Hydrological conditions	Wet
Soil Profile	O - 10 to 15 cm A – 1.5 to 2 m
Date of inspection	28.05.2023

Table 11 Factors of Safety of Soil section

S. No	Soil section	Soil			Chart no	Degree of saturation (%)	Intercept		Factor of safety (F1+F2)/ 2
		Density (g/cm^3)	Cohesion (kPa)	Angle of internal friction (°)			X (F2)	Y (F1)	
1	U	1.410	4.8946	26.791°	1	25	0.765	0.741	0.753
					3	50	0.673	0.649	0.659
					5	100	0.561	0.504	0.5321
	M	1.410	4.9135	25.63°	1	25	0.58	0.63	0.6
					3	50	0.56	0.63	0.59
					5	100	0.45	0.47	0.46
	L	1.410	32.6309	21.054°	1	25	1.40	1.28	1.34
					3	50	1.20	1.13	1.16
					5	100	1.05	1.132	1.09

5 Summary and Conclusion

The detailed study mainly involves the stability analysis of rock and soil slopes on the recent slide that occurred on the Kokalthorai to Kotagiri road. The rock mass character was evaluated using the rock mass rating (RMR) technique. No rock mass is exposed in the Class-I category; that is a very good rock. Section J1 falls in the class II category, i.e., Good Rock, whereas sections J2 and J3 fall in class III, that is, Fair Rock. The rock slope stability analysis used slope mass rating (SMR). In this technique, the above results of RMR are used as input parameters. The analyses show that sections fall under class IV, indicating unstable conditions. Based on kinematic analysis, the possible pattern of failures, such as planar or wedge, is identified. Out of 3 rock slope joints selected for detailed stability analysis, one discontinuity is fulfilling planar failure conditions, and the other 2 joints are in wedge failure conditions. Planar analysis, FOS is greater than one in fully saturated conditions and unsafe for other conditions. Moreover, the FoS = 1.583 is considered safe for dry conditions until the external load is acting on it. In this study area, upper, middle, and lower sections are selected for detailed stability analysis; hence, the circular failure chart (CFC) method was used. CFC analysis indicates that the slopes are unstable (FOS < 1) in the case of two slope sections (U and M), while the other section (L) is stable (FOS = 1.0). Different remedial options (Anon 2012), including geotextile reinforcement techniques, would be

implemented on the soil slope, and a suitable option that provides better results in terms of safety and stability will be suggested. Passive piles can stabilize the sliding mass above the failure surface and avoid planar and wedge failure. Rock bolts enhance the jointed rock mass in the J2 and J3 Sections. They are installing rock anchors to avoid moving along discontinuity joints. In conclusion, our study not only identifies potential instability in the analyzed sections but also proposes specific remedial measures tailored to the unique conditions of each area. The outcomes of this research provide a foundation for informed decision-making and the development of effective strategies for slope stability and landslide mitigation in the Kokalthorai to Kotagiri road region.

REFERENCE

Aleotti, P, Chowdhury, R (1999) Landslide hazard assessment: summary review and new perspectives. Bulletin of Engineering Geology and the Environment. 58, 21–44. https://doi.org/10.1007/s100640050066.

American Society for Testing Materials (ASTM) (1994) Annual book for ASTM standards-construction: soil and Rocks. ASTM Publication, West Conshohocken, PA.

Anbalagan, R, Sharma, S, Raghuvanshi, TK (1992) Rock mass stability evaluation using modified SMR approach. In: 6th National Symposium on Rock Mechanics, Proceedings, 1, pp 258–268.

Anon, (1998) Bureau of Indian Standard, IS 13365 (Part 1) Quantitative classification systems of rock mass guidelines—rock mass rating (RMR) for predicting engineering properties. BIS, New Delhi.

Anon (2012). Hill Road manual. The Indian Roads Congress (IRC), Jamnagar House, New Delhi.

Beiniawski ZT (1976) Rock mass classification in rock engineering. In: Beiniawski ZT (ed.) Exploration for rock engineering, Proceedings of the symposium exploration. Rock Engineering, pp 97–10, Johannesburg.

Beiniawski ZT (1979) The geo-mechanics classification in rock engineering applications. In: Proceedings of the 4th International Congress Rock Mechanics, 2, pp 41–48, Montreux, Balkema, Rotterdam.

Beiniawski ZT (1989) Engineering rock mass classifications. Wiley, Chichester.

Beiniawski, ZT (1973) Engineering classification of jointed rock masses. Trans South Af. Inst. Civil Eng. 15(12), 335–344.

Hoek E, Bray JW (1981) Rock Slope Engineering. Stephen Austin and Sons Limited Publishers, Hertford.

International Society of Rock Mechanics (ISRM) (1981) Rock characterization, testing, and monitoring. In: Brown ET (ed.) ISRM suggested methods. Pergamum Press, Oxford.

Kannan, M, Saranaathan, SE, Anabalagan, R (2017) Soil slope stability analysis by circular failure chart method, A case study in Bodi—Bodimettu Ghat section, Theni district, Tamil Nadu. India. Int. J Earth Sci. Eng. 10(6), 1163–1167. https://doi.org/10.21276/ijee.2017.10.060

Maksud Kamal, A. S. M, Farhad Hossain, Bayes Ahmed, Md. Zillur Rahman, Peter Sammonds, (2023) Assessing the effectiveness of landslide slope stability by analyzing structural mitigation measures and community risk perception. Natural Hazards. 117, 2393–2418 https://doi.org/10.1007/s11069-023-05947-6

Prasanna Venkatesh, S, Rajeshwara Rao, N, Saranaathan, S. E (2023) Geomechanical and Kinematic Stability Analysis of Unstable Slopes (Near 9th km Stone) on Palani—Kodaikanal Ghat Section in Tamil Nadu. Landslides: Detection, Prediction, and Monitoring: Technological Developments. Cham: Springer International Publishing, pp 127–144.

Romana, M (1985) New adjustment ratings for application of Bieniawski classification to slopes. In: Proceedings of the international symposium on the role of rock mechanics in excavations for mining and civil works. International Society of Rock Mechanics, pp 49–53, Zacatecas.

Saranaathan, S.E, Kannan, M (2017) SMR and Kinematic analysis for Slope Instability along Bodi - Bodimettu Ghat section, Tamil Nadu, India. Journal of the Geological Society of India. 89, 589 - 599. https://doi.org/10. 1007/s12594-017-0648-1.

Saranathan, E, Kanagasabai, S, Kannan, M, Venkatraman, GK (2014) A geotechnical assessment of slope stability condition at Lovedale Club Slide, Lovedale, The Nilgiris, Tamil Nadu. Int. J Earth Sci. Eng. 7(1), 251–259.

Sharma, R. K, Mehta, BS, Jamwal, CS (2013) Cut slope stability evaluation of NH-21 along Natayan–Gambhrola s.ection, Bilaspur district, Himachal Pradesh, India. Natural Hazards. 66, 249–270. doi:

10.1007/s11069-012-0469-x.
Tariq Siddique, M. E. A., Mondal, S. P., Pradhan, M, Salman, M, Sohel1, (2020) Geotechnical assessment of cut slopes in the landslide-prone Himalayas: rock mass characterization and simulation approach. Natural Hazards. 104, 413–435 https://doi.org/10.1007/s11069-020-04175-6.